AD_____

GRANT NO: DAMD17-94-J-4126

TITLE: Development of Efficient Dynamic Magnetic Resonance Imaging Methods With Application to Breast Cancer Detection and Diagnosis

PRINCIPAL INVESTIGATOR(S): Jill M. Hanson

CONTRACTING ORGANIZATION: University of Illinois
Urbana, Illinois 61801

REPORT DATE: September 1995

TYPE OF REPORT: Annual

PREPARED FOR: Commander
U.S. Army Medical Research and Materiel Command
Fort Detrick, Maryland 21702-5012

September 1995 Annual (9/1/94-8/31/95)

Development of Efficient Dynamic Magnetic Resonance Imaging Methods With Application to Breast Cancer ... DAMD17-94-J-4126

Jill M. Hanson

University of Illinois
Urbana, Illinois 61801

U.S. Army Medical Research and Materiel Command
Fort Detrick, Maryland 21702-5012

Approved for public release; distribution unlimited

The purpose of this predoctoral fellowship research project is to use edge information with the Reduced-encoding Imaging by Generalized-series Reconstruction (RIGR) technique to improve temporal and spatial resolution in dynamic contrast-enhanced magnetic resonance imaging of the breast. Towards this goal, a multiresolution technique was selected for the edge detection, and several methods of incorporating the boundary information into the generalized-series model were investigated. As an offshoot from the original proposal, a novel technique for utilizing the additional information available from a second high-resolution reference image was developed. This Two reference RIGR (TRIGR) method can effectively improve the temporal resolution of dynamic images without sacrificing spatial resolution and is well-suited for application to dynamic contrast-enhanced magnetic resonance imaging of the breast.

magnetic resonance imaging, dynamic imaging, contrast-enhanced dynamic imaging, generalized-series 40

Unclassified Unclassified Unclassified Unlimited

FOREWORD

Opinions, interpretations, conclusions and recommendations are those of the author and are not necessarily endorsed by the US Army.

____ Where copyrighted material is quoted, permission has been obtained to use such material.

____ Where material from documents designated for limited distribution is quoted, permission has been obtained to use the material.

____ Citations of commercial organizations and trade names in this report do not constitute an official Department of Army endorsement or approval of the products or services of these organizations.

____ In conducting research using animals, the investigator(s) adhered to the "Guide for the Care and Use of Laboratory Animals," prepared by the Committee on Care and Use of Laboratory Animals of the Institute of Laboratory Resources, National Research Council (NIH Publication No. 86-23, Revised 1985).

____ For the protection of human subjects, the investigator(s) adhered to policies of applicable Federal Law 45 CFR 46.

____ In conducting research utilizing recombinant DNA technology, the investigator(s) adhered to current guidelines promulgated by the National Institutes of Health.

____ In the conduct of research utilizing recombinant DNA, the investigator(s) adhered to the NIH Guidelines for Research Involving Recombinant DNA Molecules.

____ In the conduct of research involving hazardous organisms, the investigator(s) adhered to the CDC-NIH Guide for Biosafety in Microbiological and Biomedical Laboratories.

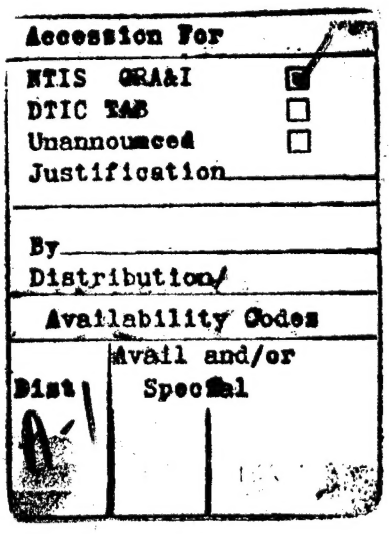

Jill M Hanson 9/28/95

PI - Signature Date

Table of Contents

4 Introduction

This fellowship research project focuses on improving the temporal and spatial resolution in dynamic contrast-enhanced magnetic resonance imaging (MRI) of the breast. Dynamic contrast-enhanced MRI has been investigated as a possible means for non-invasive determination of the benign or malignant status of a breast tumor due to the differential rate of enhancement following injection of a contrast agent (1–9). In order to capitalize on the time of greatest differentiation between malignant and benign lesions, a sequence of images of the breast must be acquired during the first 1 or 2 minutes following contrast injection (10,11), leading to a requirement for high temporal resolution. In addition, high spatial resolution in 3 dimensions is imperative to allow the visualization of very small tumors with complete coverage of the breast. High signal-to-noise ratio (SNR) is necessary so that noise does not interfere with the differentiation between the malignant and benign enhancement rates.

However, with conventional MRI techniques, since each of the dynamic images is collected independently, the requirements for increasing the temporal and spatial resolutions are conflicting. For example, if N encodings are collected for each image where TR is the time to collect one encoding and Δk is the spatial frequency step between encodings, the spatial resolution will be $\frac{1}{N\Delta k}$, but the temporal resolution will be limited to NTR which may not be acceptable for large N.

To overcome this problem with conventional MRI, several methods have emerged to reduce the number of dynamic encodings needed per dynamic image. Perhaps the most well-known are the Reduced-encoding Imaging by Generalized-series Reconstruction (RIGR) (12, 13) and Keyhole (14, 15) techniques which are characterized by the same data acquisition scheme (Fig. 1). Both methods acquire a single high-resolution reference image with a series of reduced dynamic encodings.

The main difference between the methods is in the reconstruction of the dynamic images. Keyhole uses a Fourier series based approach. The high frequency encodings from the reference data set are appended to the low frequency dynamic encodings to create a full data set which is then inverse Fourier transformed to arrive at the dynamic image. Although the method has been applied to dynamic breast imaging (16,17), it has

many problems which can cause improper diagnosis due to missed lesions (18). There is the potential for data inconsistency between the reference and dynamic data sets which could lead to image artifacts. This is especially important in contrast-enhanced imaging because the inflow of the contrast agent causes an increase in the overall intensity level as well as the intensity in the enhancing areas. In addition, Keyhole can only track dynamic changes at low resolution (19, 20). This can easily be seen by looking at the reconstruction equation for I_{diff}, which is the difference image between the reference image and a dynamic image or, effectively, an image of the dynamic changes:

$$I_{\text{diff}}(x) = \sum_{n=-N/2}^{N/2-1} [d_{\text{dyn}}(n\Delta k) - d_{\text{ref}}(n\Delta k)]\, e^{-i2\pi n\Delta k x}. \qquad [1]$$

Since N is the number of dynamic encodings, it can be seen that the dynamic changes are reproduced at low resolution with Keyhole. Since the changes are the object of interest in dynamic contrast-enhanced MRI, Keyhole is not well suited for this application.

Although RIGR uses the same number of dynamic encodings, RIGR can reconstruct the dynamic images with a higher spatial resolution than is possible with a Fourier based approach. This is because the basis functions of the generalized series model contain high-resolution information from the reference image. This has important ramifications in the tracking of dynamic changes as can be seen below in the reconstruction equation for the difference image I_{diff}:

$$I_{\text{diff}}(x) = \sum_{n=-N/2}^{N/2-1} c_n \underbrace{I_{\text{ref}}(x) e^{-i2\pi n\Delta k x}}_{\text{basis functions}} = \sum_{n=-N/2}^{N/2-1} c_n \varphi(x). \qquad [2]$$

The importance of this difference will be demonstrated in the figures in the completed research section of this report.

The purpose of this fellowship research project is to use edge information with the RIGR technique to improve the temporal and spatial resolution in contrast-enhanced dynamic imaging of the breast. The motivation for this is that the RIGR technique tends to bias the contrast of the dynamic image towards that of the reference image. By using only the edge information from the reference image, this problem should be alleviated. Towards this goal, the problems of edge extraction and the incorporation of

the boundary information into the RIGR algorithm were investigated. As the project evolved, a novel method for utilizing the additional information from a second high-resolution reference image was developed. These topics will be covered in the body of this report, and areas for future work will be discussed in the conclusion.

5 Completed Research

The two project areas of boundary extraction and the utilization of this edge information in the RIGR algorithm will be discussed in this section. In addition, the new TRIGR technique which arose from the work on this project will be covered. Since it is the dynamic changes that are of interest, the results will be presented as images of the dynamic changes. Both Keyhole and the original RIGR algorithm will be included for comparison purposes.

To test the methods developed during this research, a breast simulation was designed which has four lesions surrounded by breast "parenchyma" (see Fig. 2). Only two of the lesions are visible pre-contrast to allow the effects of the boundary determination to be shown. One of these tumors and one of the others enhance rapidly, and the other two enhance more slowly, modeling malignant and benign lesions, respectively. In addition, the parenchyma has a gradual increase in intensity as occurs in contrast-enhanced MRI. The size and location of the lesions can be changed as well as the rate of enhancement of each region to test an algorithm's spatial resolution and ability to track the time course of enhancement. Since the dynamic images and the time evolution of signal in each pixel is known exactly in these simulated images, it will be easy to judge the performance of an algorithm.

5.1 Edge Extraction

The first area that was addressed was the extraction of the edge information from the reference image. Two methods were investigated for doing this: wavelet edge detection and the closely related multiresolution edge detection. Both schemes detect edges at several scales which is advantageous because structures of different sizes may be of importance in an image. However, the concept of *scale* is different in the two transforms.

For the wavelet edge detector, the idea of scale is tied to the size of the edge itself. This results in detecting wider edges as the scale of the wavelet gets larger. With the multiresolution edge detector, the concept of scale relates to both physical proximity and greyscale "closeness" between regions enclosed by a boundary.

5.1.1 Wavelet Edge Detection

Wavelets are a new form of basis functions that show promise for application to many problems in signal processing (21–23), magnetic resonance imaging (24–29), etc. They have generated a lot of interest due to the fact that they can be chosen to be localized in both frequency and time (or space), unlike the Fourier basis functions which are of infinite length in time (or space.) In addition, wavelets can be chosen to be orthonormal with a high number of vanishing moments. These properties promise the ability to represent a signal or image with fewer components than is possible with Fourier methods. The application of wavelets that relates to this project is the ability of some types of wavelets to perform edge detection (30–32). It has been shown (31) that a wavelet which is the derivative of a "smoothing function" can, in effect, perform multiscale edge detection. This is because the local extrema at each scale of the wavelet transform detail image using such a wavelet is the derivative of the image smoothed at that scale.

The Mallat wavelet edge detector was tested on several MRI images to see how it behaved. An example is shown in Fig. 3. The original image is image (a), and images (b)-(h) show the detail image of the wavelet transform at seven scales. For the purpose of edge detection, the detail images would be thresholded at an appropriate level to retain only the wavelet transform maxima. Although thresholding reduces the edges due to noise variations, it also causes more segments of the desired edges to be lost. This was not done here to show that the edges are quite broken using this edge detector even before the thresholding, and there are important boundaries that this wavelet edge detector missed, such as the upper boundary of the large tumor. The reason for this dropout is that the wavelet edge detector makes an implicit assumption about the shape of the edge. It can only detect edges that have a similar shape to that of the chosen wavelet. However, there is no way to know *a priori* the shape of an edge in an MR image. For this reason, we turned our attention to the multiresolution edge detection

approach which does not make any *a priori* assumptions about the shape of the edge, but lets the boundaries emerge from the interactions between the pixels.

5.1.2 Multiresolution Edge Detection

The multiresolution edge detection approach (33, 34) is similar to the wavelet edge detection approach in that it can give boundaries at various scales. However, the multiresolution edge detector computes the "force" between all pixels in the image and uses the resulting force field to determine the edges. As such, it does not impose an *a priori* model of the shape of the edge. The force or attraction between two pixels depends on both the grey level difference and the physical proximity between them. This is based on the observation that two points that are close together are more likely in one region than two points that are distant from each other. In addition, a high grey level contrast between two pixels indicates more strongly the possibility that they are in separate regions than two pixels that have similar grey levels. At different resolutions, the grey level and physical closeness that is required for a group of pixels to comprise a region is different.

Figure 4 shows the results of applying this algorithm to the same image as in Fig. 3. Image (a) is the original MR image, and images (b)-(h) show the edges detected at progressively coarser scales. For our purposes, the multiresolution edge detector seems to capture the boundaries of the regions better than the wavelet edge detector while maintaining the benefits of edges at various scales. The boundaries are more continous which is what would be expected in an MR image since tumors, etc., have continuous boundaries. In addition to an image of the edges, the program, which was written by Narendra Ahuja and Mark Tabb, can also output an image with the regions replaced by their average values or by the region number. This additional information can be valuable for the selection of the "most important" boundaries in an image.

5.2 Using the Edge Information

As mentioned before, the RIGR algorithm uses the generalized series model for the reconstruction of the dynamic images:

$$I_d(x) = \sum_{n=-N/2}^{N/2-1} c_n I_{\text{ref}}(x) e^{-i2\pi n\Delta kx} = \sum_{n=-N/2}^{N/2-1} c_n \varphi(x). \qquad [3]$$

The edge information must be used to create a new I_{ref} which contains the boundaries from the high-resolution reference image, but the contrast from the dynamic data. In this way, information about the dynamic changes is contained not only in the coefficients, c_n, but also in the basis functions of the generalized series. The key step in this project is to incorporate the edge information into the RIGR algorithm in the best possible way.

Given that the edges have been extracted from the reference image, they were used to create a 1D boxcar model for each phase encoding to which the data was fit to determine the appropriate amplitudes for each boxcar region using the equation:

$$d(n\Delta k) = \sum_{m=0}^{M-1} a_m w_m \text{sinc}(w_m n\Delta k) e^{-i2\pi n\Delta k x_m} \qquad [4]$$

where $d(n\Delta k)$ is the data, M is the number of regions, and w_m and x_m are the width and center, respectively, of a region. Both the dynamic data and the corresponding encodings from the reference data set were fit to this model. This information was used in three different ways.

Method 1

In this method, the reference image that was used was simply the boxcar model that was fitted to the dynamic data. In other words, the reference image had the edges from the reference image, but the image intensity in each region was the fitted mean of the dynamic signal. Although this idea seemed good, it resulted in a loss in spatial resolution since all of the high frequency variations in the reference image were removed.

Method 2

For this reason, a different approach was tried in which both fitted boxcar models were used. The mean value of each region from the reference and dynamic fitted boxcar models were used to scale the mean intensity level in the high-resolution reference image. In this way, the mean contrast in the reference image was closer to that of the dynamic image, but the higher frequency variations were allowed to remain in the reference image.

This significantly improved the results over the previous approach.

Method 3

Additional improvement was gained by using the fitted means for the dynamic and reference data to scale the signal in the regions of the high-resolution reference image, rather than scaling only the mean. The results of using this method on the breast simulation are shown in Fig. 5. Image (a) and (b) are the pre-contrast reference and dynamic image, respectively. Image (c) is the difference image between (a) and (b) and is the "gold-standard" for comparison with the next three images. These three images were reconstructed using 128 phase encodings while the next three images were reconstructed using 16 dynamic phase encodings. Images (d) and (e) were reconstructed using the Keyhole and the original RIGR methods, respectively. Image (f) was reconstructed from the new RIGR algorithm with edge information. Significant improvement from the use of edge information can be seen in the upper two lesions of image (f). As expected, the lower two lesions are not as well resolved since the reference image has no information about the boundaries of these two lesions.

Figure 6 shows profiles through the upper two tumors of the images in Figure 5. The enforcement of the edge constraints has led to a reduced smearing of the edge between the two regions as well as a flatter intensity profile through each region.

The application of the method to data from rats with breast cancer provided by Dr. Erik Wiener of Dr. Paul Lauterbur's group is shown in Fig. 7. Images (a)-(c) are the reference image, the dynamic image and the difference between the two images, respectively. These three images were reconstructed using 256 phase encodings. In this case, a post-contrast reference image is used to provide the edge constraints for the regions. Images (d)-(f) show the difference image reproduced using only 8 phase encodings with the Keyhole method, the original RIGR method and the modified RIGR method, respectively. Profiles through the large enhancing tumor for each of these images are shown in Fig. 8. The improvement due to the use of edge information is not as apparent here as in the breast simulation. This indicates that we need to determine a better way to use the boundary information for a real, noisy image.

These results generated a poster presentation at the 3rd Annual Meeting of the Society of Magnetic Resonance held in August at Nice, France (see Appendix A).

5.3 Two-reference RIGR

An effective method for improving the temporal and spatial resolution for a sequence of dynamic images developed as an offshoot from this research project. The two reference RIGR (TRIGR) method utilizes the additional information available from a second high-resolution reference image to improve the quality of the reconstructed dynamic images. This method is motivated by the observation that, in many dynamic imaging applications, it is possible to obtain two high-resolution reference images - one for the baseline state and another for the active state. In the case of contrast-enhanced dynamic imaging of the breast, the baseline reference would be a high-resolution pre-contrast image. The active reference would be a high-resolution post-contrast image, taken after the dynamic imaging period when the contrast agent is strongly visible in the slice.

The TRIGR method uses the data acquisition scheme illustrated in Fig. 9. A high-resolution baseline reference image is acquired where the number of phase encodings is dictated by the spatial resolution requirements. This is followed by a series of reduced dynamic encodings, where the number of encodings is chosen to give the desired temporal resolution. The third component is a high-resolution active reference image. It is important to note that the active reference image need not be acquired after the dynamic imaging period. All that is required is that the active reference image indicate the areas of change from the baseline reference image. For some applications, it may be beneficial to acquire multiple reference images at various points in the experimental protocol and then use the appropriate two images for the reconstruction of a given dynamic image. This multiple reference version may be appropriate for breast imaging if, for example, it is desired to monitor the shape of the contrast agent washout curve (35,36).

Reconstruction of the dynamic images is accomplished using the generalized series model as with the original RIGR algorithm except that information about the dynamic changes is built into the basis functions by using a difference reference image. Specifically, the reconstruction steps are:

1. Construct the difference reference image by reconstructing the baseline and active reference images using the traditional Fourier method with the full set of encodings and subtracting the complex images.

2. Create the dynamic difference data by subtracting from the dynamic data the corresponding encodings of the baseline reference image, namely

$$d_{\text{diff}}(x) = d_{\text{dyn}}(k) - \hat{d}_{\text{baseline}}(k) \qquad [5]$$

where $d_{\text{dyn}}(k)$ is the dynamic data and $\hat{d}_{\text{baseline}}(k)$ represents the corresponding part of the baseline reference encodings.

3. The TRIGR model then becomes:

$$I_{\text{diff}}(x) = I_{\text{ref}}(x) \sum_{n=-N/2}^{N/2-1} c_n e^{i2\pi n \Delta k x} \qquad [6]$$

where $I_{\text{ref}}(x)$ is the difference reference image of step 1 and N is the number of dynamic encodings. The coefficients c_n are obtained by fitting the difference data of Eq. (5) to the following equation to maintain data consistency (12)

$$d_{\text{diff}}(m) = \sum_{n=-N/2}^{N/2-1} c_n d_{\text{ref}}(m-n) \qquad [7]$$

where $d_{\text{ref}}(m-n)$ is the difference data created by subtracting the baseline and active reference data sets. Plugging these coefficients into Eq. 6 will yield the reconstructed dynamic difference image.

4. If the dynamic image itself is desired, it can be generated by adding the complex dynamic difference image of step 3 to the baseline reference image, ie:

$$I_{\text{dyn}}(x) = I_{\text{baseline}}(x) \quad + \quad I_{\text{diff}}(x) \qquad [8]$$

where $I_{\text{baseline}}(x)$ is reconstructed using the standard Fourier technique with the full set of encodings.

This modification to the RIGR algorithm has several benefits. In the original RIGR algorithm, the basis functions were derived from either a pre-contrast or post-contrast reference image. However, the contrast in either of these images may not accurately represent the dynamic changes, which could lead to image artifacts. In the TRIGR method, information about the dynamic changes is built into the basis functions by using a difference reference image. This new reference image should more closely reflect the dynamic changes and, thus, lead to a better dynamic image.

In addition, the fitting to ensure data consistency is performed using the difference data. This allows the parameters of the generalized series model to represent only the dynamic changes, not the static parts of the image. This should lead to a more faithful reproduction of the dynamic changes.

Fig. 10 shows the application of this technique to the breast simulation. Images (a) and (b) are the pre-contrast and post-contrast references, respectively. Image (c) is the difference image between the dynamic image (not shown) and the pre-contrast image. This is the image we are trying to reconstruct. These three images were all reconstructed using 128 phase encodings. The next three images show the difference image reconstructed using only 8 phase encodings with three different methods. Images (d) and (e) were reconstructed using Keyhole and the original RIGR algorithm, respectively. Image (f) was reconstructed using the TRIGR method. The improvement of (f) over (d) or (e) can easily be seen. Note in particular the improved reconstruction of the lower two lesions as compared to the original RIGR algorithm. This is due to the fact that the difference reference image contributes *a priori* information about those lesions that is not present in the pre-contrast reference image.

Figure 11 shows images of a rat with breast cancer made with data from Dr. Erik Wiener. Images (a), (b), and (c) are the pre-contrast, post-contrast and dynamic change image (difference between the dynamic image (not shown) and the pre-contrast image), respectively, reconstructed using 256 phase encodings. Images (d), (e) and (f) were reconstructed using only 8 phase encodings with Keyhole, the original RIGR method, and the new TRIGR method. The increase in image quality in (f) is obvious. Since only 8 phase encodings were used, as opposed to 256, this would lead to a 32-fold time savings over conventional Fourier imaging.

The TRIGR algorithm generated a conference talk at the 3rd Annual Meeting of the Society of Magnetic Resonance (see Appendix A), and a manuscript has been submitted for publication in *Magnetic Resonance in Medicine* (see Appendix B). In addition, TRIGR processing has been included in the V2.0 release of the V software package (see Appendix C) so other researchers can test the algorithm.

6 Conclusions

Given the success that we have had so far, we expect to be able to meet the goals stated in the original fellowship research project proposal. In addition, since the TRIGR method has shown so much promise and is well-suited for application to dynamic contrast-enhanced MRI of the breast, we plan to add the following items to this project:

1. Incorporate edge information with the TRIGR method. This includes determining the best way to extract the relevent edge information from the reference images as well as the incorporation problems discussed with the regular RIGR processing.

2. Test the method using the breast simulation to determine the attainable temporal and spatial resolutions and the ability of the method to track the enhancement curves of different regions versus lesion size, number of dynamic phase encodings, etc.

3. Test the methods using MRI data to see how it works on real data.

7 References

[1] S. H. Heywang, A. Wolf, E. Pruss, T. Hilbertz, W. Eiermann, W. Permanetter, MR imaging of the breast with Gd-DTPA: Use and limitations. *Radiology* **171**, 95–103 (1989).

[2] W. A. Kaiser, MR imaging examination of both breasts within 6 minutes: Technique and first results, in "Proc., RSNA, 75th Annual Meeting, Chicago, 1989", p. 164.

[3] W. A. Kaiser, MR imaging of the breast: Optimal imaging technique, results, limitations and histopathologic correlation, in "Proc., RSNA, 75th Annual Meeting, Chicago, 1989", p. 230.

[4] W. A. Kaiser, O. Mittelmeier, Breast-tissue differentiation by MRI: Results of 361 examinations in 5 years, in "Tissue Characterization in MR Imaging, Springer-Verlag, 1990", pp. 254–257.

[5] W. A. Kaiser, MRM promises earlier breast cancer diagnosis. *Diagnostic Imaging*, 88–93 (1992).

[6] S. E. Harms, D. P. Flamig, K. L. Hesley, W. P. Evans, Magnetic resonance imaging of the breast. *Mag. Res. Quarterly* **8**, 139–155 (1992).

[7] S. E. Harms, D. P. Flamig, Breast: visualizing Ca not seen by radiography. *Body MRI*, 20–24 (1993).

[8] S. E. Harms, D. P. Flamig, MR imaging of the breast. *J. Magn. Reson. Imaging* **3**, 277–283 (1993).

[9] J. P. Stack, O. M. Redmond, M. B. Codd, P. A. Dervan, J. T. Ennis, Breast disease: Tissue characterization with Gd-DTPA enhancement profiles. *Radiology* **174**, 491–494 (1990).

[10] W. A. Kaiser, E. Zeitler, MR imaging of the breast: Fast imaging sequences with and without Gd-DTPA, preliminary observations. *Radiology* **170**, 681–686 (1989).

[11] B. A. Porter, J. P. Smith, MRI enhances breast cancer detection and staging. *MR*, 18–26,35 (1993).

[12] Z.-P. Liang, P. C. Lauterbur, Improved temporal/spatial resolution in functional imaging through generalized series reconstruction, in "Works-in-Progress Proc., SMRI, 10th Annual Meeting, New York, 1992", p. S15.

[13] Z.-P. Liang, P. C. Lauterbur, An efficient method for dynamic magnetic resonance imaging. *IEEE Trans. Med. Imaging* **13**, 677–686 (1994).

[14] J. J. van Vaals, H. H. Tuithof, W. T. Dixon, Increased time resolution in dynamic imaging, in "Proc., SMRI, 10th Annual Meeting, New York, 1992", p. 44.

[15] J. E. Bishop, I. Soutar, W. Kucharczyk, D. B. Plewes, Rapid sequential imaging with shared-echo fast spin-echo MR imaging, in "Works-in-Progress Proc., SMRI, 10th Annual Meeting, New York, 1992", p. S22.

[16] D. B. Plewes, J. Bishop, I. Soutar, E. Cohen, Errors in quantitative dynamic three-dimensional Keyhole MR imaging of the breast. *J. Magn. Reson. Imaging* **5**, 361–364 (1995).

[17] D. E. Egerter, Keyhole imaging enhances dynamic contrast studies. *MR*, 8,13,49 (1992).

[18] J. Bishop, R. M. Henkelman, D. B. Plewes, Dynamic spin-echo imaging: Theoretical assessment and implementation. *J. Magn. Reson. Imaging* **4**, 843–852 (1994).

[19] X. Hu, On the "keyhole" technique. *J. Magn. Reson. Imaging* **4**, 231 (1994).

[20] T. A. Spraggins, Simulation of spatial and contrast distortions in keyhole imaging. *Magn. Reson. Med.* **31**, 320–322 (1994).

[21] I. Daubechies, Orthonormal bases of compactly supported wavelets. *Comm. Pure Appl. Math.* **XLI**, 909–996 (1988).

[22] S. G. Mallat, A theory for multiresolution signal decomposition: The wavelet representation. *IEEE Trans. Patt. Anal. Machine Intell.* **11**, 674–693 (1989).

[23] S. G. Mallat, Multifrequency channel decompositions of images and wavelet models. *IEEE Trans. Acoust., Speech, Sig. Proc.* **37**, 2091–2110 (1989).

[24] J. B. Weaver, Y. Xu, D. Crean, D. M. Healy, Wavelet encoding in MR imaging, in "Proc., SMRM, 10th Annual Meeting, 1991", p. 182.

[25] J. B. Weaver, Y. Xu, D. M. Healy, J. R. Driscoll, Wavelet-encoded MR imaging. *Magn. Reson. Med.* **24**, 275–287 (1992).

[26] D. M. Healy, J. B. Weaver, Two applications of wavelet transforms in magnetic resonance imaging. *IEEE Trans. Info. Theory* **38**, 840–860 (1992).

[27] X. Hu, A. H. Tewfik, H. Garnaoui, A new wavelet based MR imaging technique, in "Proc., SMRM, 11th Annual Meeting, 1992", p. 432.

[28] I. Panych, P. Jakab, F. Jolesz, An implementation of wavelet-encoded MR imaging, in "Proc., SMRI, 11th Annual Meeting, 1993", p. 26.

[29] J. M. Hanson, Z.-P. Liang, P. C. Lauterbur, A new method for fast dynamic imaging using wavelet transforms, in "Proc., SMRM, 12th Annual Meeting, 1993", p. 712.

[30] S. Mallat, S. Zhong, Compact image coding from edges with wavelets, in "Proc., Int. Conf. Acoust. Speech Sig. Proc., Toronto, 1991", pp. 2745–2748.

[31] S. Mallat, S. Zhong, Characterization of signals from multiscale edges. *IEEE Trans. Patt. Anal. Machine Intell.* **14**, 710–732 (1992).

[32] L. jen Du, J. sen Lee, K. Hoppel, S. A. Mango, Segmentation of SAR images using the wavelet transform. *Int. J. Imag. Syst. Tech.* **4**, 319–326 (1992).

[33] N. Ahuja, A transform for detection of multiscale image structure, in "Proc., DARPA Image Understanding Workshop, 1993", pp. 893–902.

[34] N. Ahuja, A transform for detection of multiscale image structure, in "Proc., Comp. Vision Patt. Recog., New York, 1993".

[35] N. M. Hylton, S. D. Frankel, L. J. Esserman, K. Moore, E. Sickles, High resolution 3D maps of contrast enhancement patterns in breast tumors, in "Proc., SMR, 3rd Annual Meeting, Nice, France, 1995", p. 439.

[36] F. Kelcz, G. E. Santyr, G. O. Cron, Incorporation of washin and washout criteria for improvement of specificity in dynamic gadolinium-enhanced MRI of breast lesions, in "Proc., SMR, 3rd Annual Meeting, Nice, France, 1995", p. 435.

8 Appendix A - Conference Presentations

Improved RIGR Dynamic Imaging Using Explicit Boundary Constraints with Application to Breast Imaging

J.M. Hanson, Z.-P. Liang and P.C. Lauterbur
Biomedical Magnetic Resonance Laboratory and Department of Electrical and Computer Engineering
University of Illinois at Urbana-Champaign, Urbana, Illinois 61801, U.S.A.

Introduction

This paper addresses the dynamic imaging problem with application to contrast-enhanced dynamic breast imaging. Specifically, we want to develop a technique which will enable us to obtain high-resolution dynamic images using a small number of dynamic encodings. In the past few years, several groups have investigated this problem, resulting in two techniques: Reduced-encoding Imaging through Generalized-series Reconstruction (RIGR) [1] and Keyhole [2, 3]. Both techniques take a single high-resolution reference image and a small number of dynamic encodings to improve temporal resolution. The difference between the two techniques is in how they recycle the reference information. In Keyhole, the high-resolution reference information is simply pasted on the low-resolution dynamic data and inverse Fourier transformed. As recently analyzed by Spraggins [4], Keyhole can only reconstruct dynamic changes at low resolution. This problem is not encountered with RIGR which uses the generalized series model to combine the reference and dynamic information in a data consistent way. This paper presents a further improvement on RIGR which enables it to produce an image of the dynamic change at a resolution approaching that of the reference image.

Method

In dynamic imaging, the object of interest is the dynamic signal change. In order to capture these dynamic changes at high spatial resolution, we modify the original RIGR processing by explicitly building boundary information into the basis functions of the generalized series model [5].

Boundary constraints are obtained from either a single reference image or two reference images, for example, a pre-contrast and a post-contrast image. Segmentation of the images is accomplished with a multiresolution algorithm [6]. This method is based on a multiscale transform that takes into account both the grey level similarity and physical proximity between pixels to compute a force on a pixel. Based on the resulting force fields, the image is segmented into different regions at different scales. The algorithm determines the regions in an image from the interactions between pixels, avoiding the use of *a priori* models of edge geometry.

One question that is often asked is: if we build this information into the basis functions, what will happen? We have found, based on a point spread function analysis, that if the edges of the reference image exactly match the boundaries associated with the dynamic changes, the dynamic change will be reconstructed with the resolution of the reference image. If the boundary constraints are not exact, the resolution will still be improved due to the reduced width of the point spread function associated with the generalized series model.

Results and Discussion

The method was used for contrast-enhanced dynamic MR imaging on rats with breast cancer. The method showed significant improvement in difference image quality over keyhole and the original RIGR. This is illustrated in the figure below where the pre-contrast reference image (a), post-contrast reference image (b) and difference image (c) were reconstructed using 256 phase encodings. Images (d), (e) and (f) show the difference image reproduced using only 8 dynamic phase encodings with the Keyhole method, the original RIGR method and the modified RIGR method, respectively. The increase in image quality of (f) over (d) or (e) can easily be seen.

Conclusions

An improved method is proposed in this paper for fast dynamic imaging. This method provides significantly better spatial resolution for dynamic imaging than Keyhole or the original RIGR. The method is especially useful for contrast-enhanced dynamic MR imaging experiments in which high temporal and spatial resolution is desired.

Acknowledgements

Thanks to Dr. Narendra Ahuja and Mark Tabb for the multiscale segmentation program and to Dr. Erik Wiener for the contrast-enhanced dynamic imaging data. This work is supported by an Army Breast Cancer Research Program Predoctoral Fellowship (JH), the Whitaker Foundation, NSF STC grant NSF-DIR-89-20133, NIH Grants PHS-5-P41-RR05964 and 1S10RR06243, ONR grant N00014-92-J-1160, the National Center for Supercomputing Applications and the Beckman Institute.

References

[1] Z.-P. Liang and P.C. Lauterbur, *Work-in-Progress*, 10th SMRI, New York, S15, 1992.
[2] J.E. Bishop, I. Soutar, W. Kucharczyk and D.B. Plewes, *Work-in-Progress*, 10th SMRI, New York, S22, 1992.
[3] J. van Vaals, H.H. Tuithof and W.T. Dixon, *Abstract*, 10th SMRI, New York, 44, 1992.
[4] T.A. Spraggins, *Magn. Reson. Med.*, 31, 320-322, 1994.
[5] Z.-P. Liang, J.M. Hanson and P.C. Lauterbur, *2nd SMR*, 53, 1994.
[6] N. Ahuja, *Proc. DARPA Image Understanding Workshop*, 893-902, April 1993.

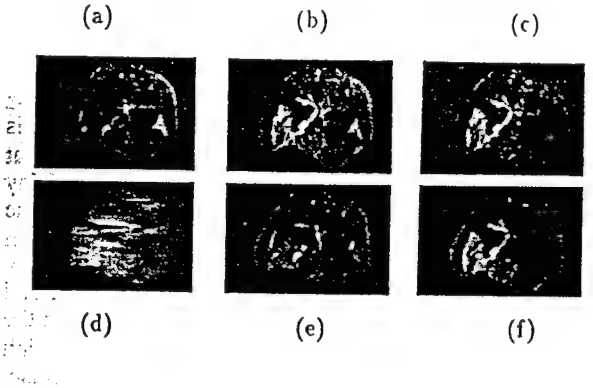

(a)-(c) pre-constrast and post-contrast reference and dynamic difference images, respectively, reconstructed with 256 phase encodings. (d)-(f) dynamic difference image reproduced with Keyhole, original RIGR and proposed method, respectively, using 8 dynamic phase encodings.

Fast Dynamic Imaging Using Two Reference Images

J.M. Hanson, Z.-P. Liang, E. Wiener and P.C. Lauterbur
Biomedical Magnetic Resonance Laboratory and Department of Electrical and Computer Engineering
University of Illinois at Urbana-Champaign, Urbana, Illinois 61801, U.S.A.

Introduction

In dynamic imaging, one is interested in reconstructing a sequence of images from the same slice or volume to monitor a process such as the enhancement due to an injected contrast agent. Several groups have been investigating the problem of providing high temporal resolution for the sequence of images while maintaining high spatial resolution. The approach used by RIGR (Reduced-encoding Imaging through Generalized-series Reconstruction) [1] and Keyhole [2, 3] is to collect a single high-resolution reference image followed by a series of reduced dynamic encodings. This paper presents two modifications to RIGR to further increase the quality of the reconstructed images: (1) using two reference images and (2) fitting the generalized series model to the difference data.

Method

The new method is motivated by the fact that in dynamic imaging the object of interest is the dynamic change. We can benefit from this by using the RIGR technique to calculate the difference image between the reference and dynamic images. This allows the parameters of the RIGR algorithm to model only the dynamic change, not the underlying high-resolution morphology, and should lead to a better reconstruction of the dynamic process. Consequently, we want to use a reference image that represents the regions of dynamic change. We do this by utilizing two reference images - one for the "baseline" state and one for the "fully active" state. In the example of contrast-enhanced dynamic MR imaging of the breast, the baseline reference is a pre-contrast high resolution image and the active reference is a high resolution image following the dynamic data sets when the contrast agent is strongly visible in the image.

The steps of the two-reference RIGR are as follows:

(1) A high-resolution baseline reference data set is acquired followed by a sequence of reduced encoding dynamic data sets and a high-resolution active reference data set.
(2) To create the difference reference image, we simply subtract the pre-contrast reference image from the post-contrast reference image.
(3) The corresponding section of the baseline reference data set is subtracted from the low-resolution dynamic data to create the dynamic difference data.
(4) The difference reference image of (2) and the dynamic difference data of (3) are processed using the RIGR algorithm. The resulting difference image can be overlaid on the baseline reference image to obtain the dynamic image.

Note that no benefit will be derived from following a similar methodology in Keyhole. If the difference dynamic data were substituted into the difference reference image, the dynamic changes between a pair of images would still be reconstructed at low resolution due to the linearity of the Fourier transform.

Results and Discussion

The method was tested on contrast-enhanced dynamic MR imaging data of rats with breast cancer. Illustrated in the figure below are the pre-contrast (a), post-contrast (b) and dynamic difference (c) images which were reconstructed using 256 phase encodings. Images (d), (e) and (f) show the dynamic difference image reproduced using only 8 dynamic phase encodings with the Keyhole method, the original RIGR method and the two-reference RIGR method, respectively. The increase in image quality of (f) over (d) or (e) can easily be seen. This improvement in difference image quality would lead to a more faithful tracking of the dynamic process.

Conclusions

A fast dynamic imaging method has been developed which utilizes two reference images to improve the quality of dynamic images produced by RIGR. In addition, RIGR is used to reconstruct the difference image to allow the model to more accurately fit the dynamic changes. The difference image can be overlaid on the baseline reference image to obtain the dynamic image if desired. The method is applicable to dynamic imaging applications in which baseline and fully active reference images can be obtained such as contrast-enhanced dynamic MR imaging.

Acknowledgements

This work is supported by an Army Breast Cancer Research Program Predoctoral Fellowship (JH), the Whitaker Foundation, NSF STC grant NSF-DIR-89-20133, NIH Grants PHS-5-P41-RR05964 and 1S10RR06243, ONR grant N00014-92-J-1160, the National Center for Supercomputing Applications and the Beckman Institute.

References

[1] Z.-P. Liang and P.C. Lauterbur, *Work-in-Progress*, 10th SMRI, New York, S15, 1992.
[2] J.E. Bishop, I. Soutar, W. Kucharczyk and D.B. Plewes, *Work-in-Progress*, 10th SMRI, New York, S22, 1992.
[3] J. van Vaals, H.H. Tuithof and W.T. Dixon, *Abstract*, 10th SMRI, New York, 44, 1992.

(a)-(c) pre-constrast reference, post-contrast reference and dynamic difference images, respectively, reconstructed with 256 phase encodings. (d)-(f) dynamic difference image reproduced using only 8 dynamic phase encodings with Keyhole, original and two-reference RIGR, respectively.

(a) (b) (c) (d) (e) (f)

V: A Software System for MR Signal Processing

H. Jiang, C. P. Hess, J. M. Hanson, C. S. Potter, and Z.-P. Liang
Department of Electrical and Computer Engineering and Beckman Institute for Advanced Science and Technology
University of Illinois at Urbana-Champaign, Urbana, IL 61801, U.S.A.

Introduction

With the emergence of new complex signal processing algorithms for spectral data quantification, constrained image reconstruction, functional MRI data analysis, and multidimensional data visualization, a unified processing platform is necessary for rapid technology transfer from developers to users. The development of V as a general-purpose, public-domain software system for MR signal processing is our attempt to address this problem [1]. While V is not a comprehensive package which includes every known algorithm, it provides a flexible system structure for easy incorporation of new functions. It is our hope that other research groups will participate in its further developments and will adopt it as a vehicle for algorithm exchange and application.

System Overview

V is an interactive processing environment specifically designed for MR dynamic imaging, spectroscopy, and spectroscopic imaging experiments. Structurally, it has five major interdependent modules: (a) a command-line user interface, (b) working unit, (c) kernel and application functions, (d) I/O unit, (e) on-line documentation and examples. Functionally, it is similar to an earlier software system, viewit, developed at the National Center for Supercomputing Applications (NCSA) [2], in that it can be viewed as a "scientific calculator" for multidimensional arrays with extra "buttons" for a variety of MR processing functions (see Table I). Its interactive processing capability also resembles that of other general-purpose signal processing software such as Khoros [3]. Unlike Khoros, it can support data of arbitrary dimension, an especially important feature for MR data processing.

Special Features

Functionality

A unified data format is used in V to facilitate both data interchange among the existing V routines and the development of new modules. The basic storage unit in V is the register, which contains raw data, dimension information, labels for identification, and data type. Registers are stored in a stack whose size varies dynamically as more space become necessary for processing, and there is no limit to the number of data dimensions or registers. This makes V useful for simultaneous processing of data derived from experiments using multiple protocols or for analyzing different spatial or temporal slices from the same experiment.

A powerful command-line interface with on-line documentation provides a user-friendly working environment. Operations on the registers in the stack and their contents are performed through *calling interfaces*, which serve as liaisons between the user and low-level processing. For each V function, there is one calling interface. When a calling interface is active, it may also invoke a particular *library function* to process the data. In addition, a large pool of routines from LINPACK, LAPACK, EISPACK and other public domain libraries are available in V.

In addition to the rich collection of general purpose signal and image processing functions, V also contains a set of functions implementing some of the recently-developed constrained reconstruction and time-domain spectral analysis techniques. In the area of constrained reconstruction, for example, functions are available to perform processing using the RIGR (Reduced-encoding Imaging through Generalized-series Reconstruction), SLIM (Spectroscopic Localization by IMaging), GSLIM (Generalized SLIM), and half-Fourier methods. For spectral data processing, a collection of time-domain fitting algorithms including LPSVD and HSVD is provided.

Visualization is possible in the MIT X11 window environment. To maximize the software portability, visualization is implemented through software interface to other public domain display utilities. xv is used to display two-dimensional images or plots of 1D data. In many applications like functional imaging and cardiac cine imaging, it is necessary to display an image sequence as a movie so an interface to the public domain MPEG players (mpeg_encode and mpeg_play) is also present in V.

Extendibility and Portability

V is designed to facilitate the incorporation of newly-developed or often-used functions. Existing software routines written by users can be built into the kernel with minimum modification. While calling interfaces must be written exclusively in C, library functions may be written in any programming language. With this capability, it is hoped that V will serve not only as a research tool but also as a convenient means for distributing software among the MR research community.

Particular care has been taken in the development of V to ensure minimal hardware, software library and language requirements. While V has been tested only on SUN, IBM, HP and SGI workstations, the distribution includes portable source code which should compile on almost any hardware platform.

Conclusion

We have developed a software system for unified MR signal processing. V is being provided free to the public and is available via anonymous ftp from *v.brl.uiuc.edu* (128.174.211.48). In the past year, this system has already been utilized by several research groups. With further development, it may become an effective tool for the exchange and application of complex algorithms developed by different groups in the MR community.

Acknowledgements

This work was supported in part by grants from the NIH, NSF, and ONR.

References

[1] C. P. Hess, H. Jiang, Z.-P. Liang, *NCSA Tech. Rep.*, TR028, 1994.
[2] C. S. Potter, P. J. Moran, *SPIE Conf. Biomed. Image Proc. III and Three-Dim. Micros.*, 1660, 1992.
[3] K. Konstantinides, J. R. Rasure, *IEEE Trans. Image Proc.*, 3, 243, 1994.

TABLE I. *Abbreviated List of V Functions*

Data Manipulation: dimension reordering, scaling, extracting, translation, dimension reflection, redimensioning, zero padding, constant value fill, multidimensional mosaic, data replacement
Spectroscopy: SLIM, GSLIM, automatic baseline correction, HSVD, LPSVD, parameter-based synthesis and extrapolation, DC offset removal
Reconstruction: RIGR, POCS, parametric methods, windowing and filtering, n-D Fourier transform
Math: Addition, subtraction, modulus, phase, linear scaling, random data generation, wavelet transforms
Input and Output: 2D/3D plotting, static and temporal image sequence visualization, multiple I/O formats

9 Appendix B - Manuscripts

Fast Dynamic Imaging Using Two Reference Images

Jill M. Hanson*, Zhi-Pei Liang*, Erik C. Wiener, Paul C. Lauterbur*

Biomedical Magnetic Resonance Laboratory, Electrical and Computer Engineering Department*, Beckman Institute for Advanced Science and Technology
University of Illinois at Urbana-Champaign
Urbana, Illinois 61801

Abstract

This paper presents a fast dynamic imaging method which is characterized by the acquisition of two high-resolution reference images and a sequence of low-resolution dynamic data sets. Image reconstruction is accomplished using a generalized series based algorithm. Experimental results demonstrate that dynamic images with high temporal resolution can be obtained while maintaining excellent spatial resolution. This method will be useful for a variety of dynamic imaging applications including contrast-enhanced dynamic imaging and functional brain studies.

I Introduction

Many MRI applications such as contrast-enhanced dynamic imaging and functional brain studies involve the collection of a time series of images of the same slice or volume to monitor a dynamic process. In order to capture the details of the dynamic process, it is important to obtain high temporal resolution while maintaining high spatial resolution. However, with conventional Fourier imaging, the requirements for increased time resolution and spatial resolution are conflicting. Since each of the dynamic images is acquired independently, the temporal resolution possible is limited by the number of spatial encodings applied.

Two methods which have recently been proposed for improving the temporal resolution of a sequence of dynamic images are RIGR (Reduced-encoding Imaging through Generalized-series Reconstruction) (1–5) and Keyhole (6–13). The techniques are similar in that they both acquire a single high-resolution reference image with a series of reduced dynamic encodings. However, Keyhole uses a Fourier transform based approach for the reconstruction of the dynamic images. The high frequency data from the reference image is simply pasted onto the low-resolution dynamic encodings to create a full data set. This data set is then inverse Fourier transformed to arrive at the dynamic image. Image artifacts can occur as a result of data inconsistency between the reference and dynamic data sets. In addition, Keyhole can only reconstruct a low-resolution version of the dynamic changes (14, 15). On the other hand, the RIGR algorithm uses the generalized series model to reconstruct the dynamic images. Information from the reference image is built into the basis functions of the model which allows it to track the dynamic process with greater resolution than is possible using Fourier reconstruction techniques with an equivalent number of dynamic encodings. This paper presents a

modified RIGR technique which uses the additional information from a second reference image to improve spatial and temporal resolution in the dynamic images.

II Method

Compared to the original RIGR method, the proposed method is characterized by two distinguishing features: (1) the collection of two reference data sets and (2) the application of the generalized series model to the difference data sets, resulting in direct reconstruction of the dynamic signal variations. This method is motivated by the consideration that, in many dynamic imaging applications, it is possible to obtain two high-resolution reference images: one for the "baseline" state and another for the "active" state. In the example of contrast-enhanced dynamic imaging of breast cancer, where the aim is to track the changes that occur in the breast for several minutes following the injection of a contrast agent, the baseline reference would be a high-resolution pre-contrast image. The active reference would be a high-resolution post-contrast image taken after the dynamic data sets when the contrast agent is strongly visible in the image.

Data acquisition for the proposed method is characterized by the following three steps:

1. Acquire a high-resolution baseline reference image where the number of phase encodings is chosen to satisfy the spatial resolution requirements.

2. Acquire a series of low-resolution dynamic data sets where the number of phase encodings per set is chosen to give the desired temporal resolution.

3. Acquire a high-resolution active reference image. Note that this image can be acquired in the middle of the dynamic encodings if that is better for a given application. All that is required is that the active reference image indicate the areas of change from the baseline reference image. In some situations, it may be preferable to obtain reference images at various points during the experimental procedure and then use the appropriate two reference images for each dynamic image.

Reconstruction of the dynamic images is accomplished using the generalized series model with a reference image reflecting the areas of change in the sequence of images. Specifically, the reconstruction steps are:

1. Construct the difference reference image by reconstructing the baseline and active reference images using the traditional Fourier method with the full set of encodings and subtracting the complex images.

2. Create the dynamic difference data by subtracting from the dynamic data the corresponding encodings of the baseline reference image, namely

$$d_{\text{diff}}(x) = d_{\text{dyn}}(k) - \hat{d}_{\text{baseline}}(k) \tag{1}$$

where $d_{\text{dyn}}(k)$ is the dynamic data and $\hat{d}_{\text{baseline}}(k)$ represents the corresponding part of the baseline reference encodings.

3. The RIGR model then becomes:

$$I_{\text{diff}}(x) = I_{\text{ref}}(x) \sum_{n=-N/2}^{N/2-1} c_n e^{i2\pi n \Delta k x} \tag{2}$$

where $I_{\text{ref}}(x)$ is the difference reference image of step 1 and N is the number of dynamic encodings. The coefficients c_n are obtained by fitting the difference data of Eq. (1) to the following equation to maintain data consistency (1)

$$d_{\text{diff}}(m) = \sum_{n=-N/2}^{N/2-1} c_n d_{\text{ref}}(m-n) \tag{3}$$

where $d_{\text{ref}}(m-n)$ is the difference data created by subtracting the baseline and active reference data sets. Plugging these coefficients into Eq. (2) will yield the reconstructed dynamic difference image.

4. If the dynamic image itself is desired, it can be generated by adding the complex dynamic difference image of step 3 to the baseline reference image, ie:

$$I_{\text{dyn}}(x) = I_{\text{baseline}}(x) \quad + \quad I_{\text{diff}}(x) \tag{4}$$

where $I_{\text{baseline}}(x)$ is reconstructed using the standard Fourier technique with the full set of encodings.

III Results

The method was tested on contrast-enhanced dynamic MR imaging of rats with breast cancer. A representative slice through an enhancing tumor in one of the rats is shown in Fig. 1. The pre-contrast and post-contrast reference images which were reconstructed using the standard Fourier method with 256 phase encodings are illustrated in (a) and (b), respectively. Image (c) shows the dynamic difference image between the dynamic image (not shown) and the baseline reference image and was reconstructed using 256 phase encodings. Images (d), (e) and (f) show the dynamic difference image reproduced using only 8 dynamic phase encodings with the Keyhole method, the original RIGR method and the two-reference RIGR method, respectively. It can be seen that (f) more closely reproduces the dynamic changes than either (d) or (e).

IV Discussion

The generalized series approach that is employed in the proposed method builds information from the reference image into the basis functions of the model. The result

is a high-resolution dynamic image since the basis functions are high-resolution. In the original RIGR algorithm, the basis functions were from either the baseline or the active reference image. However, the contrast in these reference images may not accurately reflect the dynamic changes, which could lead to image artifacts. Given that two reference images are available, we can instead build information about the dynamic changes into the basis functions by using a difference reference image. This difference reference image will more closely represent the areas of change and will lead to a better reconstruction of the dynamic changes.

Accordingly, we use the proposed algorithm to reconstruct an image of the dynamic changes rather than the dynamic image itself. (The dynamic image can then be obtained by simply overlaying the dynamic change image on the reference image.) An additional benefit of this modification is that the parameters of the generalized series model need only represent the dynamic changes, not the static parts of the image. This leads to a more faithful representation of the dynamic changes and, thus, a better dynamic image.

These expectations are realized in the experimental results that have been obtained. As shown in Fig. 1, the image reconstructed using the proposed method (f) more closely resembles the desired difference image (c) than either the Keyhole (d) or the original RIGR algorithms (e). Since the proposed method used only 8 dynamic phase encodings, as opposed to 256, this would yield a 32-fold time savings compared to standard Fourier imaging with minimal loss of image quality.

One could consider employing a similar methodology with Keyhole by appending the high frequency difference reference data to the low frequency dynamic difference data sets followed by the inverse Fourier transform. Although the resulting difference images will be high-resolution, it is easy to prove that the actual dynamic signal changes will still be reconstructed with low resolution. This behavior is similar to the single reference image case analyzed by Spraggins (14) and Hu (15); that is, no benefit is gained from the use of two reference images in this Keyhole scheme.

V Conclusion

A fast dynamic imaging method has been developed which uses two high-resolution reference images and a sequence of reduced dynamic encodings to reconstruct a time series of dynamic images. The proposed method shows improved quality of the reconstructed dynamic images as compared to both Keyhole and the original RIGR, which would lead to a more faithful tracking of the dynamic processes. The method would be useful for a variety of dynamic imaging applications such as contrast-enhanced dynamic MR imaging and functional brain studies.

VI Acknowledgments

The authors thank Carl Gregory for experimental assistance and helpful discussions. This work was supported in part by Army Grant #DAMD17-94-J-4126 (JMH)**, NIH

Grants PHS-5-P41-RR05964, NSF-RIA Award, the National Center for Supercomputing Applications, the Beckman Institute, the Servants United Foundation, and the Whitaker Foundation.

** The content of this paper does not necessarily reflect the position or the policy of the government, and no official endorsement should be inferred.

References

[1] Z.-P. Liang, P. C. Lauterbur, Improved temporal/spatial resolution in functional imaging through generalized series reconstruction, in "Works-in-Progress Proc., SMRI, 10th Annual Meeting, New York, 1992", p. S15.

[2] A. Webb, Z.-P. Liang, R. L. Magin, P. C. Lauterbur, Application of a generalized-series reconstruction algorithm to biologic MR imaging, in "Works-in-Progress Proc., SMRI, 10th Annual Meeting, New York, 1992", p. S26.

[3] Z.-P. Liang, P. C. Lauterbur, Efficient time-sequential imaging through generalized series modeling: A simulation analysis, in "Works-in-Progress Proc., SMRM, 11th Annual Meeting, Berlin, 1992", p. 4266.

[4] Z.-P. Liang, P. C. Lauterbur, An efficient method for dynamic magnetic resonance imaging. *IEEE Trans. Med. Imaging* **13**, 677–686 (1994).

[5] A. Webb, Z.-P. Liang, R. L. Magin, P. C. Lauterbur, Application of reduced-encoding MR imaging with generalized-series reconstruction (RIGR). *J. Magn. Reson. Imaging* **3**, 925–928 (1993).

[6] J. E. Bishop, I. Soutar, W. Kucharczyk, D. B. Plewes, Rapid sequential imaging with shared-echo fast spin-echo MR imaging, in "Works-in-Progress Proc., SMRI, 10th Annual Meeting, New York, 1992", p. S22.

[7] J. J. van Vaals, H. H. Tuithof, W. T. Dixon, Increased time resolution in dynamic imaging, in "Proc., SMRI, 10th Annual Meeting, New York, 1992", p. 44.

[8] M. E. Brummer, W. T. Dixon, B. Gerety, H. Tuithof, Composite k-space windows (keyhole techniques) to improve temporal resolution in a dynamic series of images following contrast administration, in "Proc., SMRM, 11th Annual Meeting, Berlin, 1992", p. 4236.

[9] R. A. Jones, O. Haraldseth, T. B. Muller, P. A. Rinck, G. Unsgard, A. N. Oksendal, Dynamic, contrast enhanced, NMR perfusion imaging of regional cerebral ischaemia in rats using k space substitution, in "Works-in-Progress Proc., SMRM, 11th Annual Meeting, Berlin, 1992", p. 1138.

[10] G. B. Pike, J. O. Fredrickson, G. H. Glover, D. R. Enzmann, Dynamic susceptibility contrast imaging using a gradient-echo sequence, in "Works-in-Progress Proc., SMRM, 11th Annual Meeting, Berlin, 1992", p. 1131.

[11] J. J. van Vaals, H. Engels, R. G. de Graaf, H. H. Tuithof, J. A. den Boer, W. T. Dixon, R. C. Nelson, J. L. Chezmar, Method for accelerated perfusion imaging, in "Works-in-Progress Proc., SMRM, 11th Annual Meeting, Berlin, 1992", p. 1139.

[12] J. J. van Vaals, M. E. Brummer, W. T. Dixon, H. H. Tuithof, H. Engels, R. C. Nelson, B. M. Gerety, J. L. Chezmar, J. A. den Boer, "Keyhole" method for accelerating imaging of contrast agent uptake. *J. Magn. Reson. Imaging* **3**, 671–675 (1993).

[13] R. A. Jones, O. Haraldseth, T. B. Muller, P. A. Rinck, A. N. Oksendal, K-space substitution: a novel dynamic imaging technique. *Magn. Reson. Med.* **29**, 830–834 (1993).

[14] T. A. Spraggins, Simulation of spatial and contrast distortions in keyhole imaging. *Magn. Reson. Med.* **31**, 320–322 (1994).

[15] X. Hu, On the "keyhole" technique. *J. Magn. Reson. Imaging* **4**, 231 (1994).

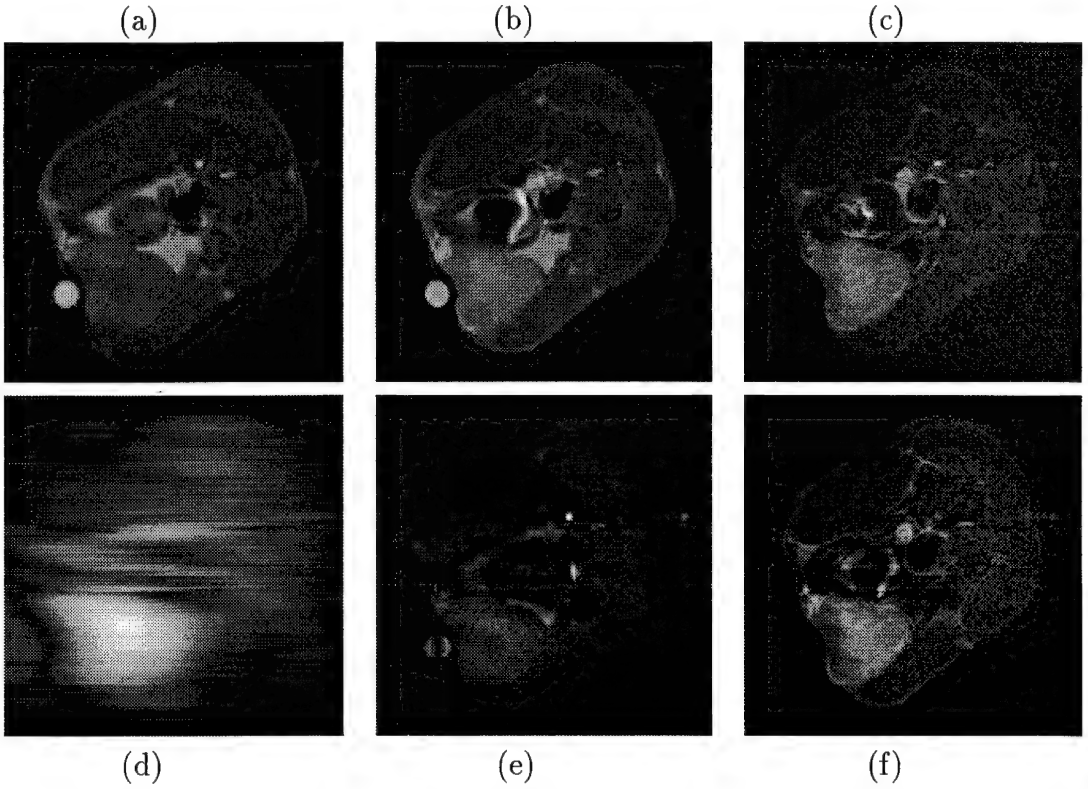

Figure 1: (a)-(c) pre-contrast reference, post-contrast reference and dynamic difference images, respectively, reconstructed with 256 phase encodings. (d)-(f) dynamic difference image reproduced using only 8 dynamic phase encodings with Keyhole, original RIGR and two-reference RIGR, respectively.

10 Appendix C - V Software Package

V is a software package for interactive multi-dimensional magnetic resonance imaging and spectroscopy reconstruction, processing and analysis which was developed by Dr. Zhi-Pei Liang's group. The V package is intended as a platform for easy distribution of functions between researchers in the MR community. V was designed so that other researchers could incorporate their own functions into the V program with minimum modification. These functions can then be easily distributed to and tested by others since a common processing platform would be used. This also would reduce duplicate programming efforts and encourage researchers to try a new method for their application.

The basic V package includes many basic functions for data manipulation and display as well as image processing algorithms such as the TRIGR algorithm developed under this research grant. V can handle real and complex multidimensional data. V also has complete documentation and on-line help. It is available via anonymous ftp at *v.brl.uiuc.edu*. Any questions or comments regarding V should be addressed to *v@mrel.brl.uiuc.edu*. This address can also be used to subscribe to a biannual newsletter that is being developed for V users.

11 Appendix D - Acronyms

BMRL - Biomedical Magnetic Resonance Laboratory

MR - Magnetic Resonance

MRI - Magnetic Resonance Imaging

RIGR - Reduced-encoding Imaging by Generalized-series Reconstruction

RSNA - Radiological Society of North America

SMR - Society of Magnetic Resonance

SMRI - Society of Magnetic Resonance Imaging

SMRM - Society of Magnetic Resonance in Medicine

SNR - Signal to Noise Ratio

TRIGR - Two reference Reduced-encoding Imaging by Generalized-series Reconstruction

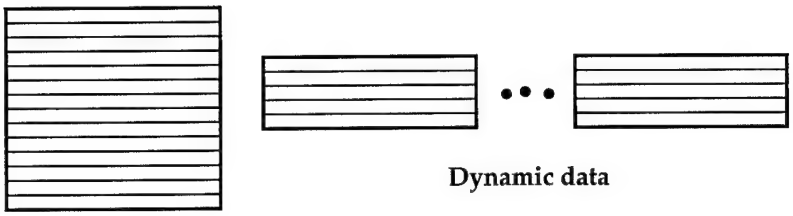

FIG. 1. Data acquisition scheme of RIGR and Keyhole: a single high-resolution reference data set is acquired followed by a series of reduced dynamic encodings.

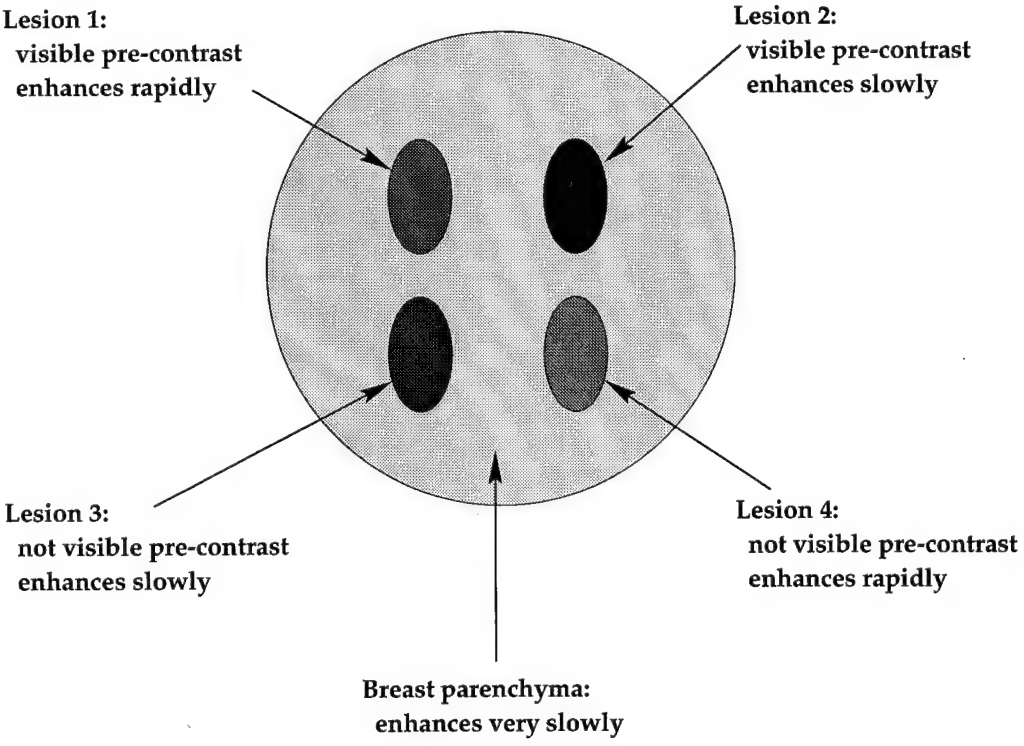

FIG. 2. Breast simulation model

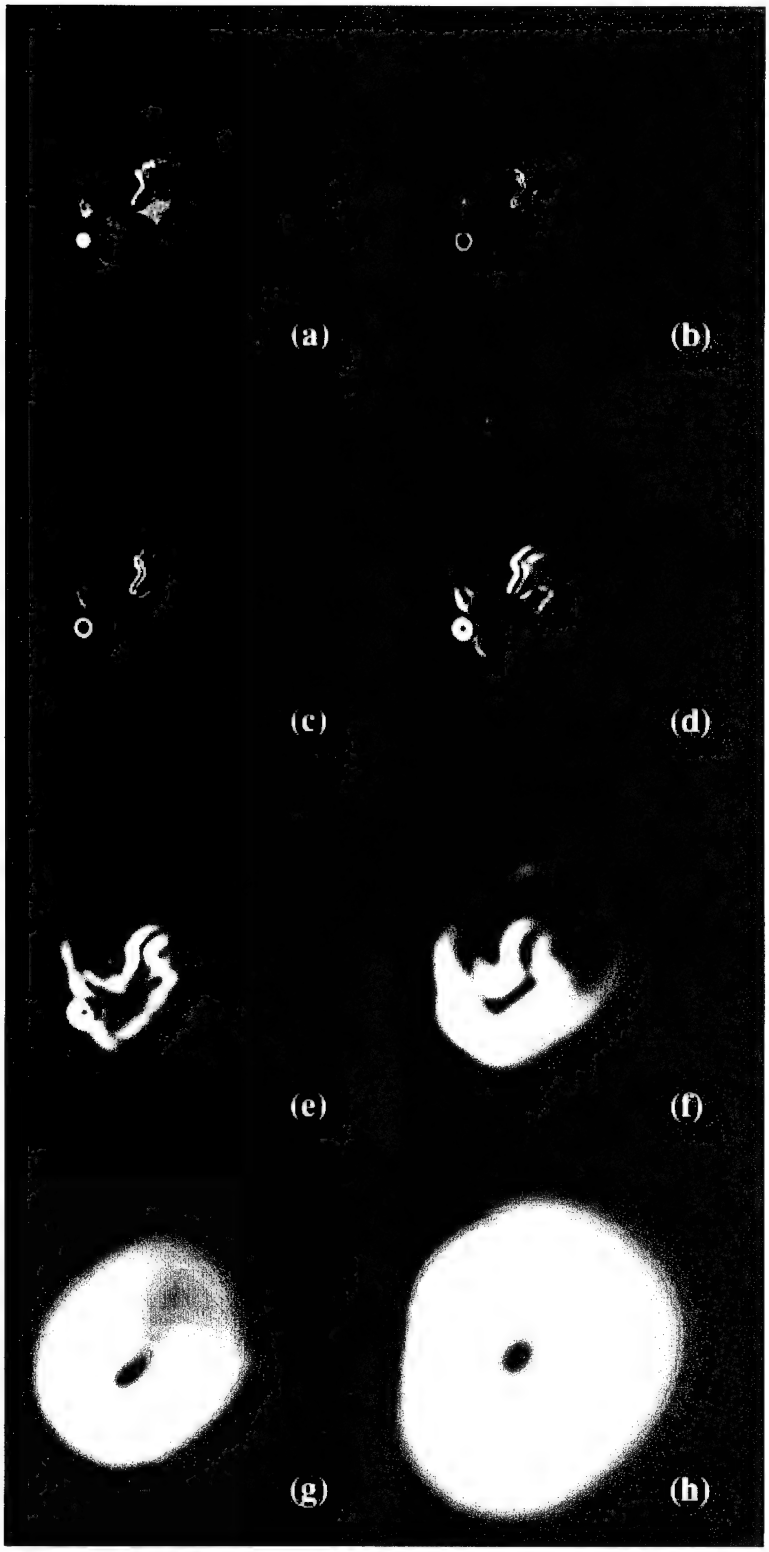

FIG. 3. Mallat wavelet edge detector: (b)-(h) edge detection results at 7 scales using the Mallat wavelet edge detector on image (a).

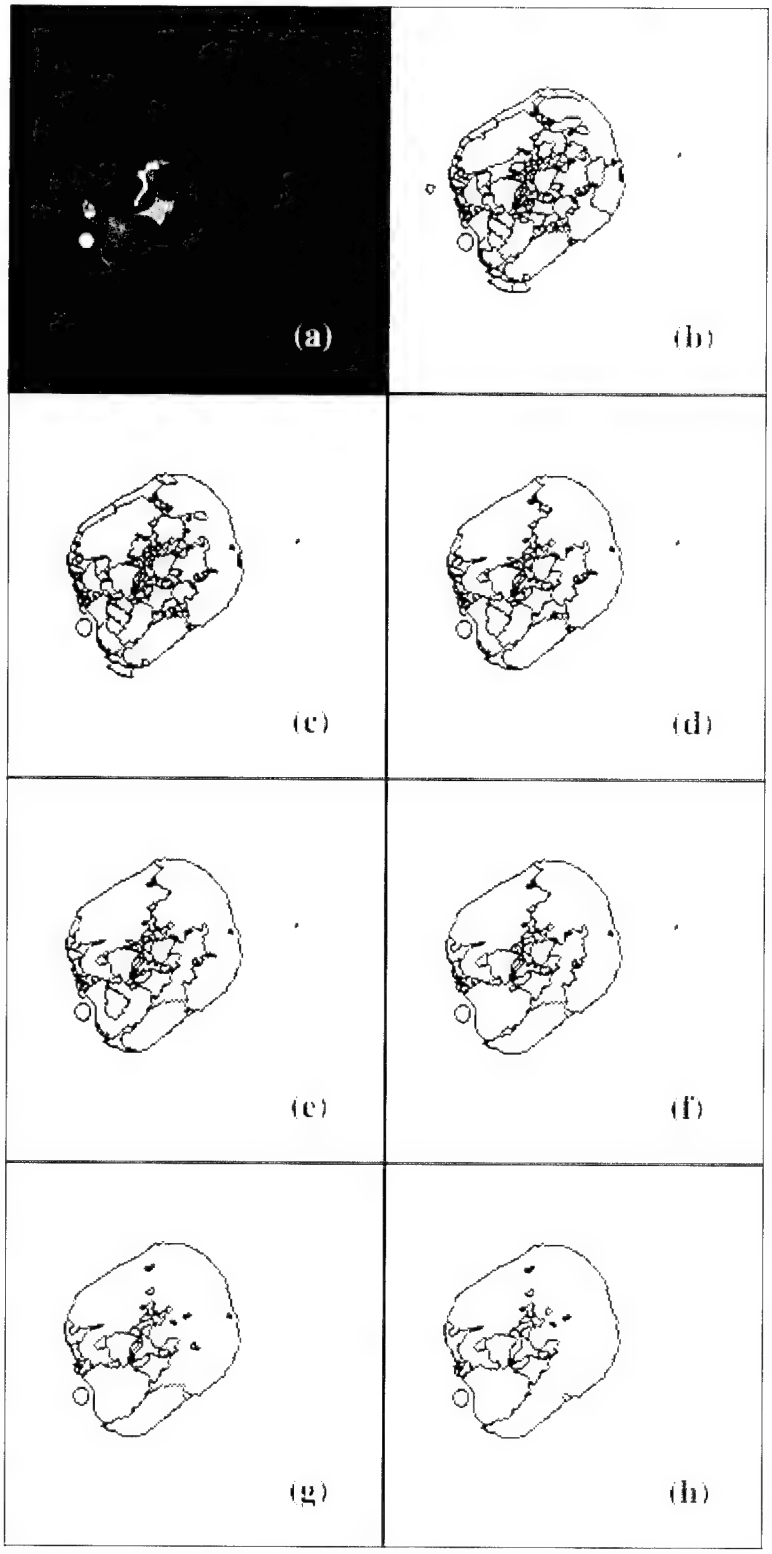

FIG. 4. Ahuja multiresolution edge detector: (b)-(h) edge detection results at 7 scales using the multiresolution edge detector on image (a).

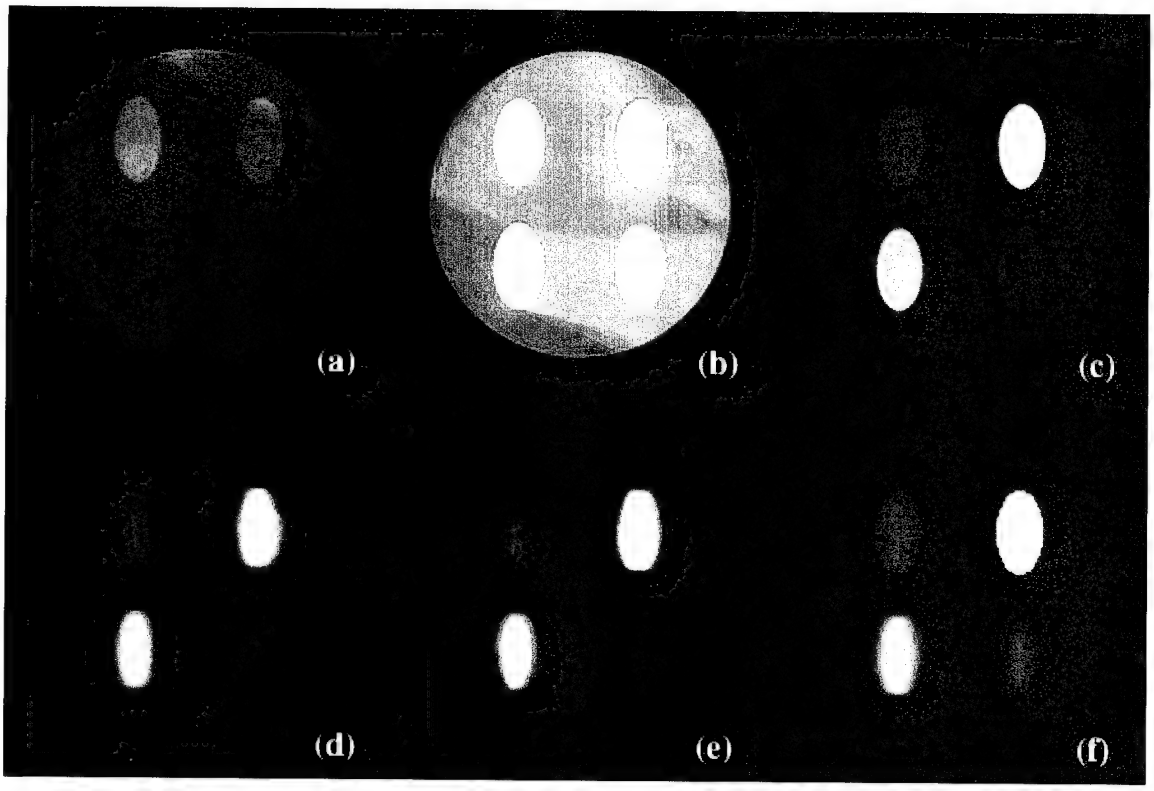

FIG. 5. Results using edge information with RIGR on breast simulation data: (a)-(c) pre-contrast reference, dynamic and difference images, respectively, reconstructed with 128 phase encodings. (d)-(f) difference image reproduced using 16 dynamic phase encodings with Keyhole, original RIGR and RIGR with edge information, respectively.

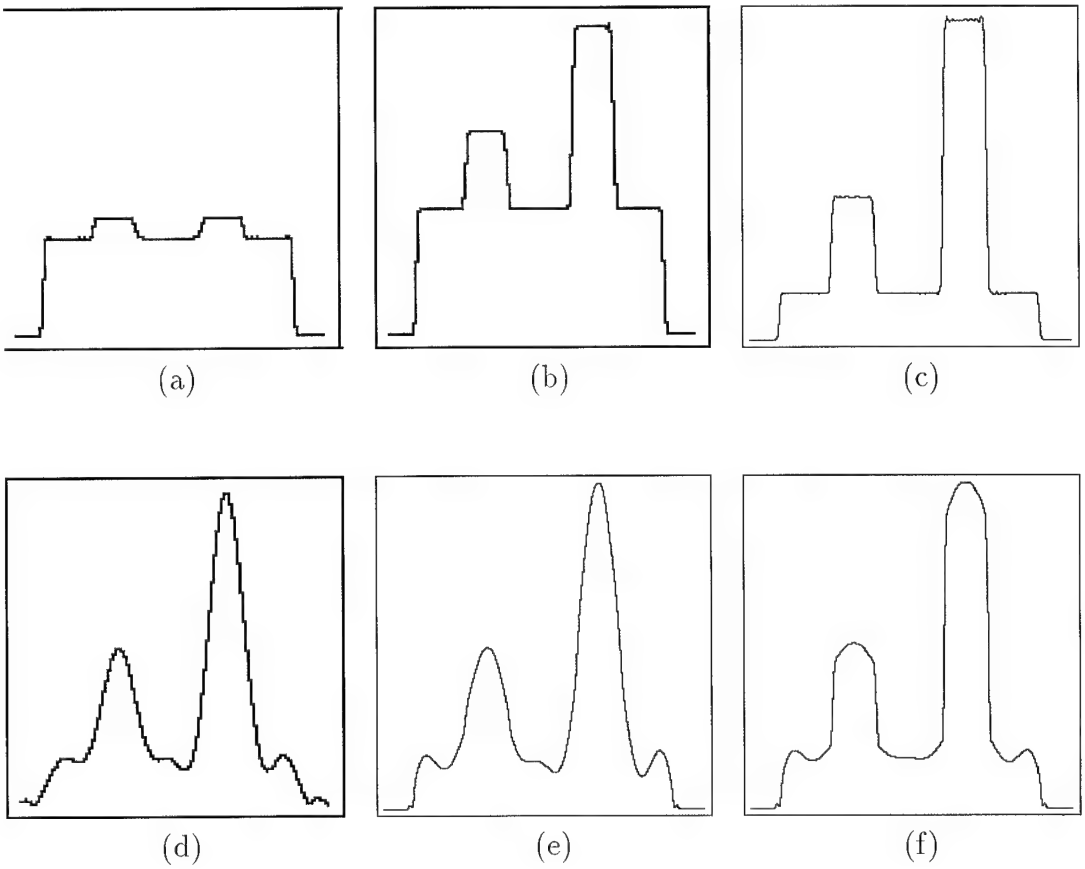

FIG. 6. Profiles through the upper two lesions of the images in Fig. 5.

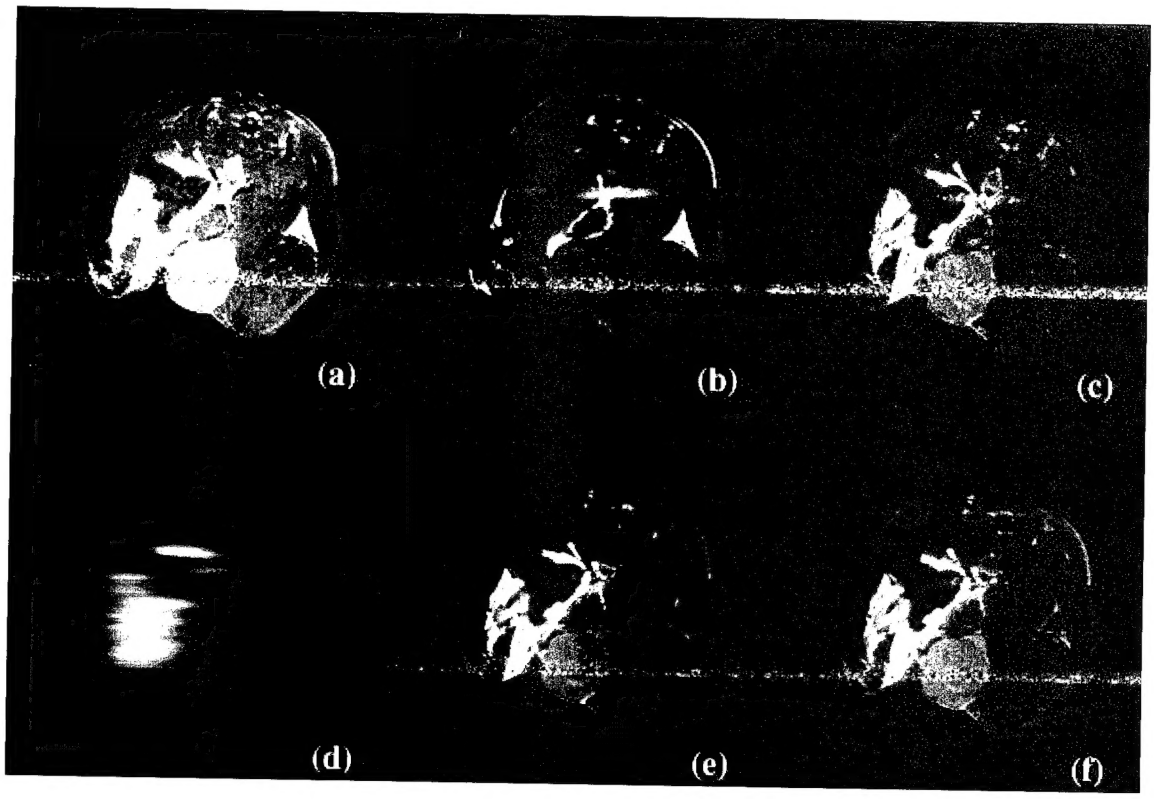

FIG. 7. Results using edge information with RIGR on a rat with breast cancer: (a)-(c) pre-contrast reference, dynamic and difference images, respectively, reconstructed with 256 phase encodings. (d)-(f) difference image reproduced using 8 dynamic phase encodings with Keyhole, original RIGR and RIGR with edge information, respectively.

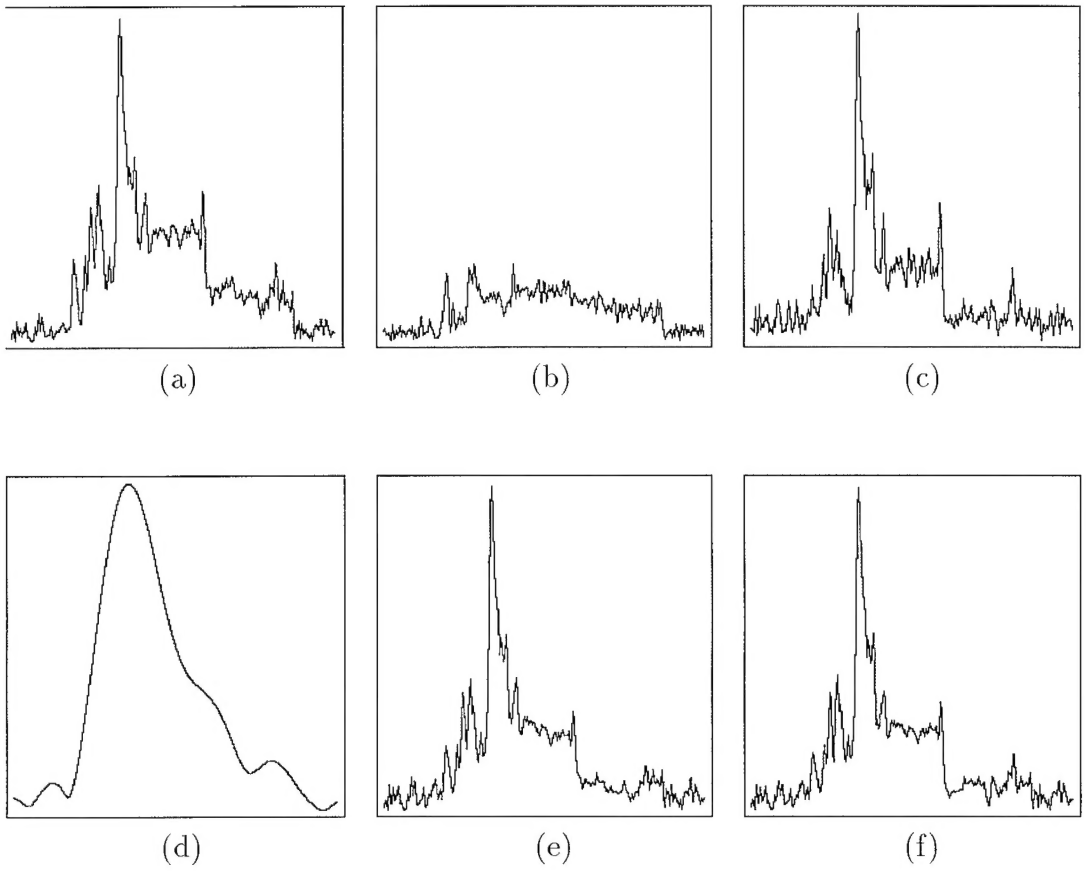

FIG. 8. Profiles through the large enhancing tumor of the images shown in Fig. 7

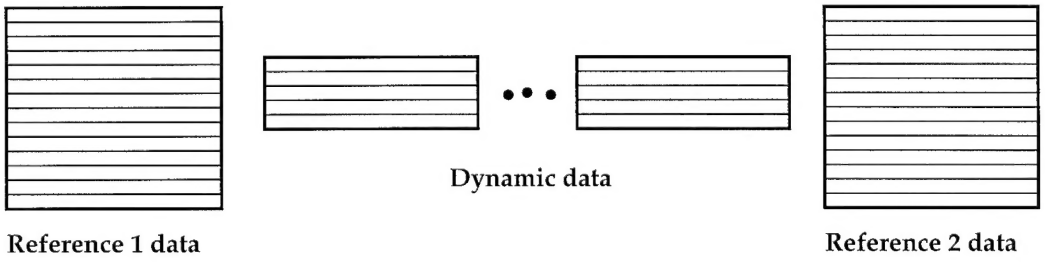

FIG. 9. The data acquisition strategy for TRIGR: two high-resolution reference images, one each for the baseline and active states, and a series of reduced dynamic encodings.

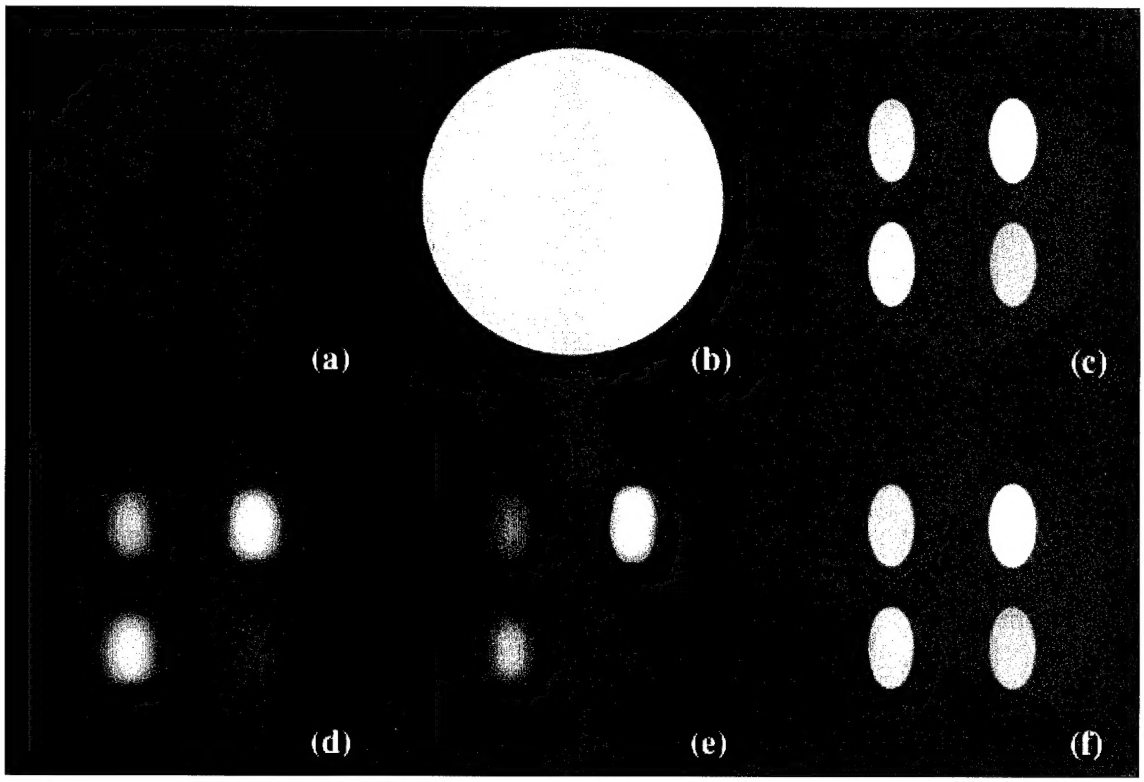

FIG. 10. TRIGR results on breast simulation data: (a)-(c) pre-contrast reference, post-contrast reference and dynamic change image (difference between a dynamic image (not shown) and the pre-contrast reference image), respectively, reconstructed with 128 phase encodings. (d)-(f) dynamic change image reproduced using only 8 dynamic phase encodings with Keyhole, original RIGR and two-reference RIGR, respectively.

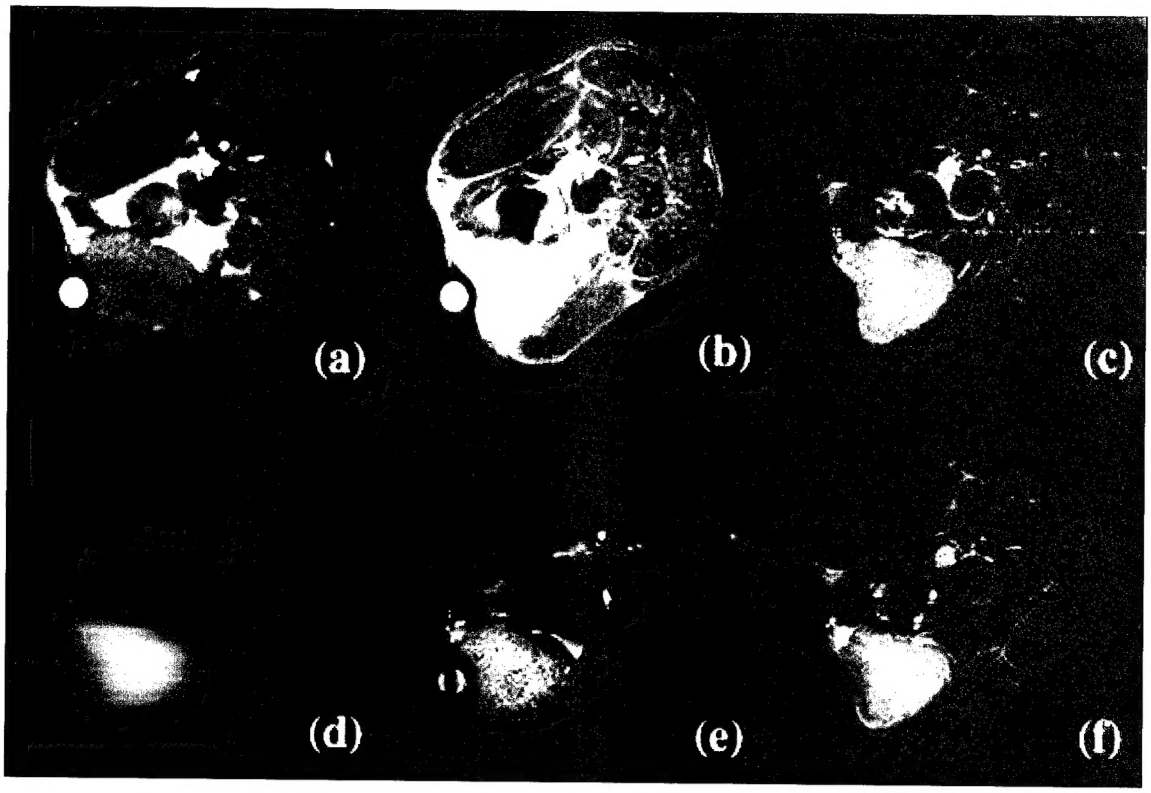

FIG. 11. TRIGR results on data from a rat with breast cancer: (a)-(c) pre-contrast reference, post-contrast reference and dynamic change image (difference between a dynamic image (not shown) and the pre-contrast reference image), respectively, reconstructed with 256 phase encodings. (d)-(f) dynamic change image reproduced using only 8 dynamic phase encodings with Keyhole, original RIGR and two-reference RIGR, respectively.